

Theoretical approach of studying human fingers modelled as inflated membranes and experimental validation of study

Andrei Călin¹, Andrei Tudor, Marilena Stoica¹, Petrică Turtoi¹

¹Department of Machine Elements and Tribology, Polytechnic University of Bucharest, Romania

E-mail: andrei.calin@upb.ro

Abstract. The human hand has evolved to become the most complex and versatile grasping and manipulation tool. The fingers play a crucial role in acquiring information about touched objects through tactile and thermal sensors. Specifically, the fingertips are densely packed with touch and thermal receptors, which have the highest concentration of cells responsible for transmitting stimuli to the brain.

Keywords: *grip, human finger, biotribology, human skin.*

Introduction

A novel approach to modeling the behavior of human fingertips has been achieved by utilizing an inflated membrane model to simulate the skin and other materials that comprise the human finger. The theoretical model was developed and compared with experimental results obtained using the CETR UMT-2 (Universal Mechanical Tester) Tribometer, which was used to perform indentation tests with various shapes and sizes of indenters. The in vivo testing method was used to capture the internal tensions present in the finger under natural conditions, resulting in a comprehensive set of data used to describe the mechanical behavior of the fingertips.

There are two types of testing used for tissues: ex vivo and in vivo. In this study, the in vivo procedure was employed to evaluate the mechanical properties of the skin in conditions that are closest to its natural state. This non-destructive method allowed only four types of tests (torsion, tension, suction, and indentation), and indenting was chosen for this study. A punch or indenter was pressed on the skin's surface, and the skin deformed in direct proportion to the applied force. The size of the punch or cup was used to highlight the properties of different layers of skin. A small diameter was used to test the upper layers, while a larger diameter was used to measure the properties in depth. Alternatively, compressed air was blown on the skin, and the deformation was measured.

This model is a refinement of the models proposed by previous researchers [3], [4], and [5].

Experimental model

The tests conducted were designed to capture the behavior of the skin and substrate in various contact conditions. The size of the indenters (diameter of 8 mm, 14 mm, and 28 mm), the force applied (3N and 5N), and the soak time (30 seconds and 2 minutes) were varied to perform a set of experiments. The step-up time for the force was fixed at 30 seconds for each test. The indenters used were manufactured out of brass, which has an elastic modulus of approximately 100 GPa, orders of magnitude greater than the skin that was tested. Therefore, the contact can be approximated as being between the human fingertip and a perfectly rigid body. The indenter used was a cylinder with the

actual part used for indenting being a hemisphere. The size of the hemisphere was varied to capture the behavior of the fingertip in contact with indenters with radii of 8, 14, and 28 mm. The tests involved capturing the creep phenomena that occurs during loading by keeping the force constant throughout the experiment and capturing the time and displacement.

Furthermore, the surface roughness of each indenter was measured to ensure that the surfaces in contact with the fingertip were similar.

Theoretical model for defining the material characteristics of human fingers

The theoretical model employed in this study used a material consisting of an envelope filled with fluid at varying pressures to simulate the different layers of the human fingertip. This layer can be filled with a pressure that alters the behavior of the entire system when subjected to an external force. The resulting shape is a 3D ellipsoid, and the contact region can be described as a degenerate ellipse, as shown in Figure 1.

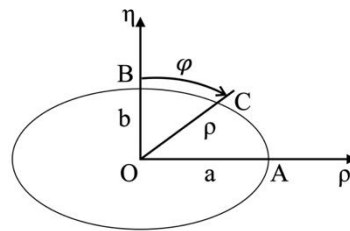


Figure 1. Ellipse coordinates

The shape of the finger in axial section can be considered to be an ellipse. Thus, the coordinates of the ellipse of semiaxes a and b with a > b can be written as a function of ρ and η.

Thus the equation for the ellipse becomes:

$$\frac{\rho^2}{a^2} + \frac{\eta^2}{b^2} = 1 \tag{1}$$

Parameter notation:

Shape parameter:

$$\varepsilon = \frac{l_0}{a} \leq 1 \tag{2}$$

Horizontal nondimensional coordinate:

$$\rho_a = \frac{\rho}{a} \tag{3}$$

Vertical nondimensional coordinate:

$$b_a = \frac{b}{a} \tag{4}$$

Thus, the equation for the ellipse becomes:

$$\frac{\rho^2}{a^2} + \frac{\eta^2}{a^2 \varepsilon^2} = 1 \tag{5}$$

Or:

$$\rho_a^2 \varepsilon^2 + \eta_a^2 = \varepsilon^2 \tag{6}$$

Thus:

$$\eta_a = \pm \varepsilon \sqrt{1 - \rho_a^2} \tag{7}$$

The coordinates of the important points on the ellipse:

$$A(a, 0) \text{ or } A(1, 0)$$

$$B(0, b) \text{ or } B(1, \varepsilon)$$

A random point on the ellipse:

$$C(\rho, \eta) \text{ or } C(\rho_a, \varepsilon \rho_a)$$

For the analysis of the various parameters of the elliptical membrane, the parametric equation of the ellipse is considered. A random point C of the ellipse is characterised by the vector radius r and angle φ measured from the vertical axis $O\eta$ expressed as $C(r, \varphi)$.

In this case, the coordinates of point C are:

$$\rho_c = r \sin \varphi \tag{8}$$

$$\eta_c = r \cos \varphi \tag{9}$$

The ellipse equation becomes:

$$\frac{\rho_c^2}{r^2} + \frac{\eta_c^2}{r^2} = 1 \tag{10}$$

$$r^2 = \frac{a^2 \varepsilon^2}{\cos^2 \varphi + \varepsilon^2 \sin^2 \varphi} \tag{11}$$

Non dimensionalising with regards to the major axis (a):

$$r_a = \frac{r}{a} = \frac{\varepsilon}{\sqrt{\cos^2 \varphi + \varepsilon^2 \sin^2 \varphi}} \tag{12}$$

$$\rho_a = \rho_{ac} = \frac{\varepsilon \sin \varphi}{\sqrt{\cos^2 \varphi + \varepsilon^2 \sin^2 \varphi}} \tag{13}$$

$$\eta_a = \eta_{ac} = \frac{\varepsilon \cos \varphi}{\sqrt{\cos^2 \varphi + \varepsilon^2 \sin^2 \varphi}} \tag{14}$$

Figure 2 (a,b,c) below show the radius and coordinates of a point on the ellipse as a function of the parameter φ for different eccentricities ε .

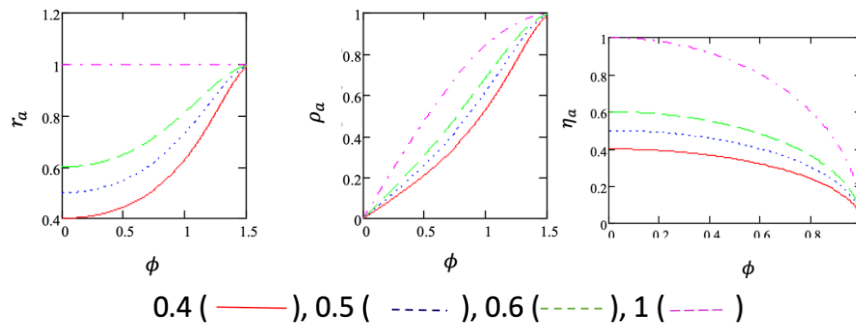


Figure 2. Radius coordinates

The finger is considered to have a truncated cone axial section of radii R_{OS} , r_{OS} and heights H_{OS} . The skin of thickness $2h_0$ is defined as an elastic membrane of the finger-bone system that envelops the tissue defined as a very viscous, incompressible fluid.

The membrane is elliptical with regards to the cone's slant height. The semiaxis of the ellipse (a, b) describe the state of the membrane at different stages. Thus, the initial state can be expressed as:

$$(a_0, b_0, \varepsilon_0 = b_0/a_0) \tag{15}$$

The inflated state can be expressed as:

$$(a, b, \varepsilon = b/a) \tag{16}$$

And the compressed stage with the use of the indenter:

$$(a_c, b_c, \varepsilon_c = b_c / a_c) \tag{17}$$

The specific extensions of the membrane in the meridional (λ_1) and circumferential (λ_2) directions are defined as the ratios between the infinitesimal linear deformations of the deformed membrane and the membrane in the initial state.

$$\lambda_1(l) = \frac{dl}{dl_0} = \frac{\sqrt{d\rho^2 + d\eta^2}}{r_0 \times d\rho} = \frac{\sqrt{\frac{d\rho^2}{d\varphi^2} + \frac{d\eta^2}{d\varphi^2}}}{r_0} = \frac{\sqrt{\rho'^2 + \eta'^2}}{r_0} = \frac{\sqrt{\rho'_a(\varphi^2) + \eta'_a(\varphi^2)}}{r_{0a}(\varphi)} \tag{18}$$

With the initial vector radius in the initial state, r_0 :

$$r_0^2 = \frac{1}{\frac{\cos^2 \varphi}{b_0^2} + \frac{\sin^2 \varphi}{a_0^2}} = \frac{a_0^2 \varepsilon_0^2}{\cos^2 \varphi + \varepsilon_0^2 \sin^2 \varphi} \tag{19}$$

$$\lambda_2(l) = \frac{r(\varphi) \sin \varphi}{a_0 \sin \varphi} = \frac{r(\varphi)}{a_0} \tag{20}$$

Assuming that the membrane (skin) is an incompressible material, the specific stretch in the direction of the membrane axis (λ_3) is:

$$\lambda_3(\varphi) = \frac{1}{\lambda_1(\varphi) \times \lambda_2(\varphi)} \tag{21}$$

Figure 3 (a, b, c) shows the same parameters ($\lambda_1, \lambda_2, \lambda_3$) that characterize the elastic deformations of the membrane, as a function of the angle φ , the shape of the initial ellipse ε_0 and the deformed state ε .

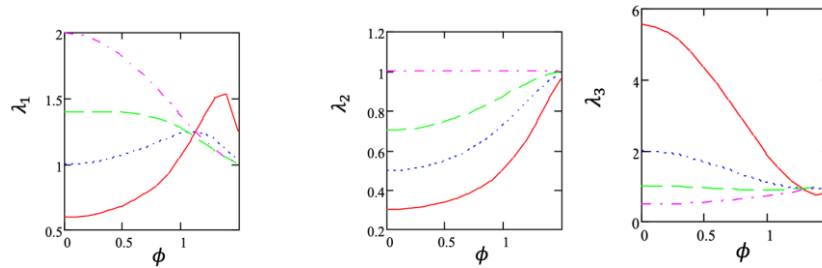


Figure 3. Elastic deformations of membrane

The invariants of the main displacements vary in the meridional (I_1) and circumferential (I_2) directions and are constant in the axial (I_3) direction (incompressible material).

Thus:

$$I_1(\varphi) = \lambda_1^2 + \lambda_2^2 + \frac{1}{\lambda_1^2 \lambda_2^2} \tag{22}$$

$$I_2(\varphi) = \frac{1}{\lambda_1^2} + \frac{1}{\lambda_2^2} + \lambda_1^2 \lambda_2^2 \tag{23}$$

$$I_3(\varphi) = 1 \tag{24}$$

Figure 4 exemplifies the evolution of these invariants in the meridional (λ_1) and circumferential (λ_2) directions on the elliptical membrane.

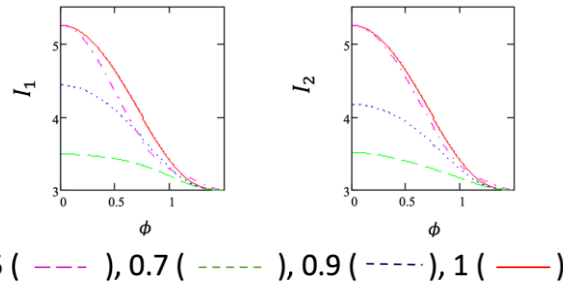


Figure 4. Evolution of invariants

For the axially symmetrical membrane, the equilibrium conditions in the tangential (meridian) and normal (latitude) directions are:

$$\frac{dT_1}{d\rho} + \frac{1}{\rho}(T_1 - T_2) = 0 \tag{25}$$

$$\kappa_1 T_1 + \kappa_2 T_2 = P \tag{26}$$

Where T_1 and T_2 are the forces per unit length of the deformed membrane, κ_1 and κ_2 are the southern and circumferential curves, P is the result of the pressures on the normal direction of the membrane. The results of the main stresses per unit length of the deformed surface of the membrane (T_1 and T_2) are determined by the specific stretches ($\lambda_1, \lambda_2, \lambda_3$) and the behavior of the membrane material (skin), characterized by the deformation energy function (W):

$$T_1 = 4h_0\lambda_3(\lambda_1^2 - \lambda_3^2) \left(\frac{\partial W}{\partial I_1} + \lambda_2^2 \frac{\partial W}{\partial I_2} \right) \tag{27}$$

$$T_2 = 4h_0\lambda_3(\lambda_2^2 - \lambda_3^2) \left(\frac{\partial W}{\partial I_1} + \lambda_1^2 \frac{\partial W}{\partial I_2} \right) \tag{28}$$

Where, W is the function of the energy of changing the shape of the membrane material per unit volume and h_0 is the semi-thickness of the membrane.

It is accepted that the skin has a behaviour similar to that of rubber, considering a material with Mooney type behaviour.

$$W = C_1(I_1 - 3) + C_2 I_2(I_2 - 3) = C_1 \left[(I_1 - 3) + \frac{C_2}{C_1} (I_2 - 3) \right] = C_1 [(I_1 - 3) + \Gamma_m (I_2 - 3)] \tag{29}$$

Where C_1, C_2 și $\Gamma_m = C_2/C_1$ are specific material parameters [J/m^3].

If the unit forces from within the membrane (T_{1a}, T_{1b}) are adimensionalised for the Mooney type material:

$$T_{1p} = \frac{T_1}{4h_0C_1} = \lambda_3(\lambda_1^2 - \lambda_3^2)(1 + \lambda_2^2\Gamma_m) \tag{30}$$

$$T_{2p} = \frac{T_2}{4h_0C_1} = \lambda_3(\lambda_2^2 - \lambda_3^2)(1 + \lambda_1^2\Gamma_m) \tag{31}$$

Figure 5 presents the adimensionalised unit forces within the elliptical membrane, for different shapes.

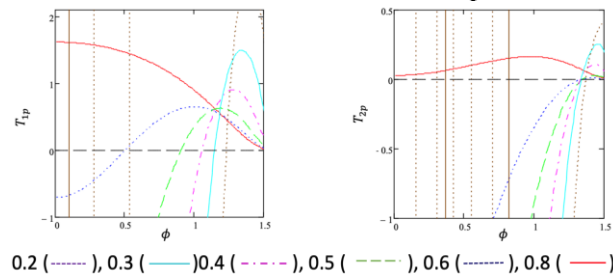


Figure 5. Unit forces

From the evolution of the forces with the current angle φ of the ellipse, it can be observed that when the ellipse is rounded from the initial shape ($\varepsilon > \varepsilon_0$), at large angles φ , the forces in the membrane are traction forces. At small angles (in the pole area), ($\varphi < 30^\circ$) and ($\varepsilon < \varepsilon_0$), the unit forces are compressive forces.

It is possible to highlight the existence of ellipse points with null forces ($T_{1a} = 0$ or $T_{1b} = 0$).

Thus, the adimensionalised main curves towards the curvature ($1/a$) (κ_1, κ_2) of the membrane evaluated using the parametric adimensionalised equation are:

$$\rho_a = \frac{\varepsilon \sin \varphi}{\sqrt{\cos^2 \varphi + \varepsilon^2 \sin^2 \varphi}} \tag{32}$$

$$\eta_a = \frac{\varepsilon \cos \varphi}{\sqrt{\cos^2 \varphi + \varepsilon^2 \sin^2 \varphi}} \tag{33}$$

$$\kappa_{1a} = \frac{-[\rho'_a \eta''_a - \rho''_a \eta'_a]}{(\rho'^2_a + \eta'^2_a)^{3/2}} \tag{34}$$

$$\kappa_{2a} = \frac{-\eta'_a}{\rho_a \sqrt{\rho_a'^2 + \eta_a'^2}} \tag{35}$$

Where $[\]'$, $[\]''$ are the derivatives of order 1 and 2 respectively in relation to the parameter φ . The variation of these principal membrane curvatures are illustrated in the Figure 6.

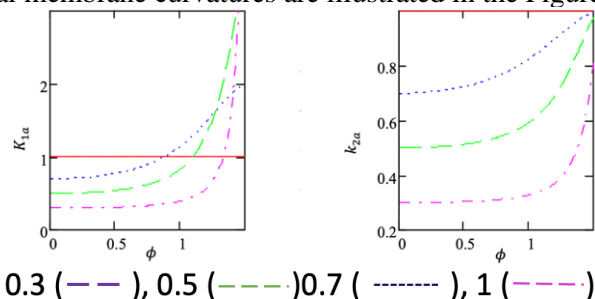


Figure 6. Variation of membrane curvature

Knowing the dependencies of unit forces (T_{1a}, T_{2a}), elliptical membrane horizontal coordinate (ρ_a) and the main curves (κ_{1a}, κ_{2a}) by the angular parameter φ , determine the appearance of the ellipse (ε).

For a planned flat curve by the parametric equation, the main curves can be determined.

Knowing the dependencies of unit forces (T_{1a}, T_{2a}), elliptical membrane horizontal coordinates (ρ_a) and the main curves (κ_{1a}, κ_{2a}) by the angular parameter φ , determine the appearance of the ellipse (ε) from the system of differential equations as a function of pressure P , initial aspect of the ellipse (ε_0), and the Mooney material coefficient (Γ_m).

The differential equation $T_1(\rho) = T_1(\rho, \varepsilon, \varepsilon_0, P, \Gamma_m)$ is a first order differential equation.

$$\frac{dT_{1P}}{d\varphi} + A(\varphi)T_{1P} = B_1(\varphi) \tag{36}$$

The solution for this equation is:

$$T_{1Pa} = \exp(-\int A(\varphi) d\varphi)(C_t + \int B(\varphi)\exp(\int A(\varphi)d\varphi)d\varphi) \tag{37}$$

In which C_t is an integration constant determined from the boundary condition:

$$T_{1P} = T_{1P0} \tag{38}$$

For any point in the incompressible fluid found on the bone; T_{1P0} is the unitary force of the fluid that binds it to the bone, experimentally determinable.

For example, $\varphi_0 = 0.001, \varepsilon_0 = 0.5, \varepsilon = 0.6, P_p = \frac{P}{4h_0C_1} = 0.008, \Gamma_m = 0.1, C_t = -0.704$. Figure 7 exemplifies the solution (T_{1Pa}) for three nondimensionalised loads P_p , with the parameters of the ellipse $\varepsilon = \varepsilon_0 = 0.5$ and the Mooney coefficient of material $\Gamma_m = 0.1$.

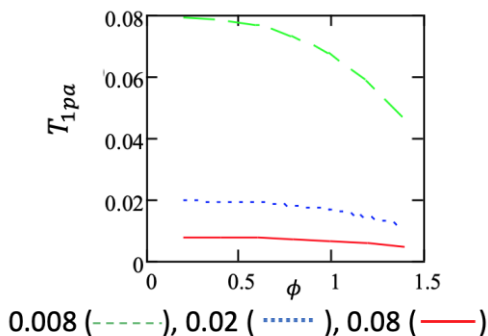


Figure 7. Example of solution

To determine the appearance of the inflated membrane, the unit force T_{1Pa} determined from the equation coincides with unit force in the membrane in the same point of the membrane (φ). From the transcendental equation:

$$T_{1Pa}(\varphi, \varepsilon, \varepsilon_0, P_p, \Gamma_m) = T_{1Pa}(\phi, \varepsilon, \varepsilon_0, P_p, \Gamma_m) \quad (39)$$

The ε_e appearance for any point is characterized by the angle φ , under the load conditions P_p , material Γ_m and the initial aspect of the membrane ε_0 .

Knowing the geometry of the inflated finger, $((\varepsilon, \rho, \eta, r))$ as a function of angle (φ) for different loads (pressure differences, P_p) initial aspect ε_0 specific to each finger and phalange and the parameter of material Γ_m the problem of skin tensions as a membrane in the model presented comes to light.

In the case of a contact between a finger and a rigid plane, prior to compression, the inflated finger as a result of the pressure difference $P = P_1 - P_2$, (the adimensionalised loading parameter P_p) is characterized by the elliptical appearance (shape) ε , semiaxis $a, b = \varepsilon a$, and the skin material as a membrane, by parameter Γ_m .

If the finger is compressed with a rigid plane with a force F_n , the shape of the finger will be B_c, A_c, A'_c, B'_c . Compression in the pole area in the direction of normal force F_n is $\overline{AD} = \delta$, and the separation angle between the flat zone ($A_c A'_c$) is Γ .

The parametric equation of the compressed finger by the rigid plane is:

$$\eta(\varphi) = \begin{cases} b - \delta, & \text{if } 0 \leq \varphi \leq \gamma \\ r_c \cos \varphi, & \text{if } \gamma \leq \varphi \leq \frac{\pi}{2} \end{cases} \quad (40)$$

$$\rho(\varphi) = \begin{cases} (b - \delta) \tan \varphi, & \text{if } 0 \leq \varphi \leq \gamma \\ r_c \sin \varphi, & \text{if } \gamma \leq \varphi \leq \frac{\pi}{2} \end{cases} \quad (41)$$

Where:

γ is the angle defined by the rigid plane and the compressed finger (compression angle);

δ is the finger compression.

The radius profile of the inflated and compressed finger is:

In the flat zone for $0 \leq \varphi \leq \gamma$

$$r_p = \frac{(b - \delta)}{\cos \varphi} = \frac{a(\varepsilon - \delta_a)}{\cos \varphi} \quad (42)$$

In the elliptical area at an angle $\gamma \leq \varphi \leq \frac{\pi}{2}$

$$r_e = \frac{a_c \varepsilon_c}{\sqrt{\cos^2 \varphi + \varepsilon_c^2 \sin^2 \varphi}} \quad (43)$$

From the continuity condition of the inflated and compressed finger profile, the large semiaxis of the deformed ellipsis a_c can be expressed as:

$$a_{ca} = \frac{a_c}{a} = \frac{(\varepsilon - \delta_a) \sqrt{\cos^2 \varphi + \varepsilon_c^2 \sin^2 \varphi}}{\varepsilon_c \cos \varphi} = \frac{\varepsilon - \delta_a}{\varepsilon_c} \sqrt{1 + \varepsilon_c^2 \tan^2 \varphi} \quad (44)$$

In the hypothesis of the incompressible fluid present in the finger, the volume in the inflated phase V_u and the inflated and compressed phase V_{uc} are equal, thus the angle of contact between a rigid plane and a modelled finger depends on the compression and deformation of the ellipse as well as the exterior force applied and the initial pressure within the fluid.

$$V_u = 2 \int_0^b \rho^2 d\eta = 2\pi \int_{\frac{\pi}{2}}^0 r^2 \sin^2 \varphi (r' \cos \varphi - r \sin \varphi) d\varphi = 2\pi a^3 \int_{\frac{\pi}{2}}^0 r_a^2 \sin^2 \varphi (r'_a \cos \varphi - r_a \sin \varphi) d\varphi \quad (45)$$

$$V_{uc} = 2 \int_0^{b-\delta} \pi \rho^2 d\eta_c = 2\pi a^3 \int_{\frac{\pi}{2}}^\gamma r_{ae}^2 \sin^2 \varphi (r'_{ae} \cos \varphi - r_{ae} \sin \varphi) d\varphi \quad (46)$$

From the volume equality, $V_{ua} = \frac{V_u}{2\pi a^3} = V_{uac} = \frac{V_{uc}}{2\pi a^3}$, the contact angle of the plane with swollen finger, γ , can be calculated for the shapes of the ellipse before, ε , and after compression, ε_c , when relative compression, δ_a , changes. This compression depends on the external force, F_n , and the fluid pressure in the finger. Figure 8 presents the schematics of the different states studied.

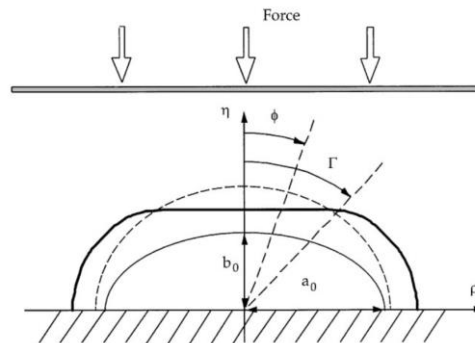


Figure 8. Representation of the axisymmetric membrane showing the uninflated, inflated, and compressed membrane [6]

Experimental results

All experiments were performed on a CETR UMT-2 (Universal Mechanical Tester) Tribometer, a versatile tribometer, for testing mechanical and tribological properties. The experimental setup is fairly simple. Three differently sized spherical tipped indenters were used (diameter of 8, 14, 28 mm). Each finger was tested with each indenter at 3 and 5 Newtons force. The force was applied using a ramp-up time of 30 seconds and a soak time of 30 and 120 seconds. The experimental setup can be seen in Figure 9.

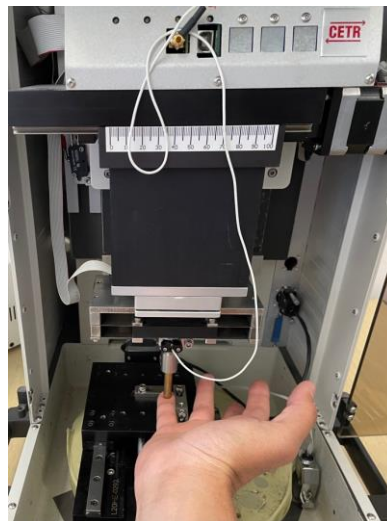


Figure 9. Experimental setup

The aim of the experiments is to measure the creep behaviour of the tissue of a human finger. This was achieved by measuring the deformation of the finger with respect to time when a constant force (3 or 5 N) is applied and maintained for a certain duration (30 or 120 seconds).

In Figures 10, 11 and 12 the general behaviour of the fingertip are shown. The results presented were gathered for the index finger using the 14 mm diameter indenter, a soak time of 30 seconds, a creep time of 120 seconds and an unloading time of 30 seconds using a 5N force.

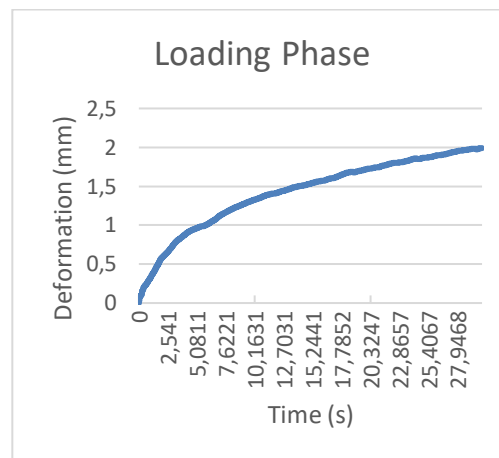


Figure 10. Loading phase (30s from 0 to 5N)

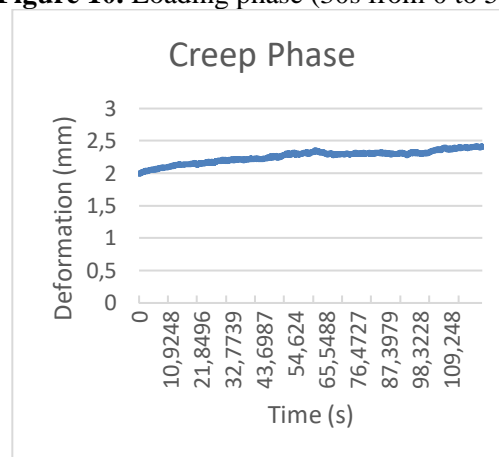


Figure 11. Creep phase (120s at 5N)

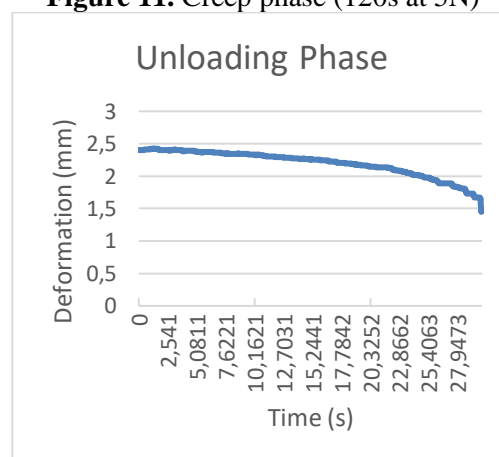


Figure 12. Unloading phase (30s from 5 to 0N)

The results presented are relevant for all fingers tested regardless of the experimental setup (indenter diameter, force applied, creep time). It can easily be observed that the majority of the deformation occurs in the loading phase. This behaviour demonstrates the classical model that involves the three phases of the stress-strain relation of human skin as discussed by [7]. This behaviour can be seen in Figure 13.

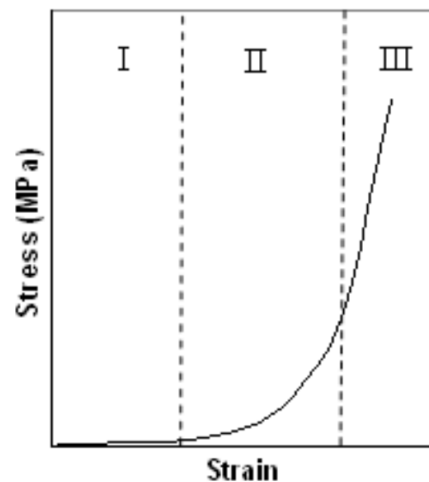


Figure 13. Stress-strain curve for skin [8]

Another interesting aspect arises by studying the deformation with respect to the force applied in the loading phase. As seen in Figure 14, the majority of the deformation occurs at a force that is less than half of the target force (5N). The force is negative because the direction of its vector is upwards.

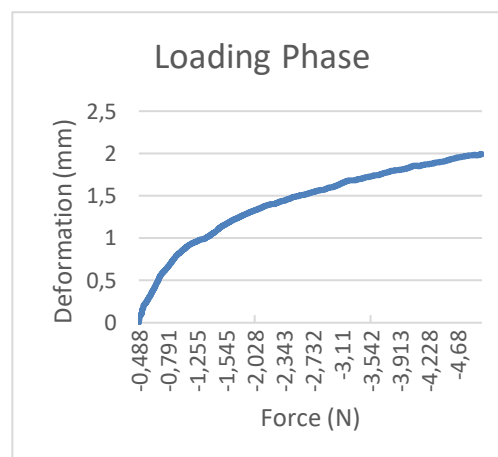


Figure 14. Loading phase (30s from 0 to 5N)

Conclusions

The results from these exploratory creep tests of fingertips indicate that the theoretical model needs to be developed further to include the relaxation phase of the phenomena as the material of the fingertip is of viscoelastic nature. Nevertheless, the model provides a simple and reasonably good quantitative method that evaluates the material characteristics of fingertips. Furthermore, the model can be also applied to other aspects such as analysis of bulk both bulk and membrane polymers.

The initial inflation causes a nonlinear distribution of stresses and stretches that are present in the membrane. Contact with the indenter makes the ellipsoid membrane to revert to a shape that is similar to the uninflated membrane at low contact forces. At higher forces, the membrane deforms up to a point and stiffens with the application of an increasing force. This can be attributed to the underlying tissues such as bone as well as the collagen fibres present in the skin.

Acknowledgment

This paper has been presented at the 10th International Conference on Tribology – BALKANTRIB '20 organised in Belgrade, on May 20-22, 2021.

References

- [1] F. M. Hendriks, D. Brokken, C. W. J. Oomens, F. P. T. Baaijens: Influence of hydration and experimental length scale on the mechanical response of human skin in vivo using optical coherence tomography. *s.l. : Skin Research and Technology*. pg. 231-241. Vol. 10, 2004.
- [2] T. Fujimura, O. Osanai, S. Moriwaki, S. Akazaki, Y. Takema: *Development of a novel method to measure the elastic properties of skin including subcutaneous tissue: New age- related parameters and scope of application*. *s.l. : Skin Research and Technology* pg. 504-511. Vol. 14, 2008
- [3] E.R. Serina, C. D. Mote, D. Rempel: A structural model of the forced compression of the fingertip pulp: *Journal of Biomechanics*, Vol. 31, pp. 639-646, 1998
- [4] D.R. Veronda, R.A. Westmann: Mechanical characterization of skin — finite deformations. *Journal of Biomechanics* 3, 111—124. 1970
- [5] A. Patil: Inflation Mechanics of Hyperelastic Membranes, Licentiate Thesis in Engineering Mechanics, 2015
- [6] E.R. Serina, C. D. Mote, D. Rempel: Force response of the fingertip pulp to repeated compression- effects of loading rate, loading angle and anthropometry, in: *Journal of Biomechanics*, Vol. 30, No. 10, 1997, pp. 1035-1040
- [7] A. E. Green, J. E. Adkins: *Large Elastic Deformations and Non-Linear Continuum Mechanics*, Oxford Clarendon Press, 1960
- [8] Brown I A: Scanning electron-microscope study of effects of uniaxial tension on human skin. *British Journal of Dermatology* 89: 383-393, 1973.